Development 134, 4437-4447 (2007) doi:10.1242/dev.010983

Spermatocyte cytokinesis requires rapid membrane addition mediated by ARF6 on central spindle recycling endosomes

Naomi Dyer[1,2,*], Elena Rebollo[3,*], Paloma Domínguez[3], Nadia Elkhatib[4], Philippe Chavrier[4], Laurent Daviet[5], Cayetano González[3] and Marcos González-Gaitán[1,6,†]

The dramatic cell shape changes during cytokinesis require the interplay between microtubules and the actomyosin contractile ring, and addition of membrane to the plasma membrane. Numerous membrane-trafficking components localize to the central spindle during cytokinesis, but it is still unclear how this machinery is targeted there and how membrane trafficking is coordinated with cleavage furrow ingression. Here we use an *arf6* null mutant to show that the endosomal GTPase ARF6 is required for cytokinesis in *Drosophila* spermatocytes. ARF6 is enriched on recycling endosomes at the central spindle, but it is required neither for central spindle nor actomyosin contractile ring assembly, nor for targeting of recycling endosomes to the central spindle. However, in *arf6* mutants the cleavage furrow regresses because of a failure in rapid membrane addition to the plasma membrane. We propose that ARF6 promotes rapid recycling of endosomal membrane stores during cytokinesis, which is critical for rapid cleavage furrow ingression.

KEY WORDS: *Drosophila*, Meiosis, Spermatogenesis, Testis

INTRODUCTION

Cytokinesis is the division of a cell into two following separation of the chromosomes during anaphase. Central spindle microtubules, the actomyosin contractile ring and their regulators, drive dramatic cell shape changes during cytokinesis (Glotzer, 2005). Cytokinesis requires coordination between the central spindle and the actomyosin contractile ring (Adams et al., 1998; Jantsch-Plunger et al., 2000; Somers and Saint, 2003). Recently, membrane trafficking has also been implicated in cytokinesis (Albertson et al., 2005; Glotzer, 2005). Membrane trafficking is necessary for the massive increase in plasma membrane surface area, and can also locally enrich specific components in the cleavage furrow plasma membrane (Bluemink and de Laat, 1973, VerPlank and Li, 2005).

The centralspindlin complex, composed of Pavarotti (Pav), RacGAP50C, and the associated Rho guanine nucleotide exchange factor (GEF) Pebble, is essential for communication between central spindle microtubules and the actomyosin contractile ring, probably by regulating the activity of the small GTPase RhoA (Somers and Saint, 2003). Active RhoA regulates actin polymerization, myosin II and citron kinase (Amano et al., 1996; Matsui et al., 1996; Yamashiro et al., 2003). Around 20 highly conserved proteins, including central spindle, actin myosin ring and RhoA pathway machinery are required for cytokinesis in multiple systems (Glotzer, 2005). However, recent RNAi screens have repeatedly identified membrane-trafficking components necessary for cytokinesis (Echard et al., 2004; Eggert et al., 2004; Skop et al., 2004).

[1]Max Planck Institute of Molecular Cell Biology and Genetics, Pfotenhauerstrasse 108, 01307 Dresden, Germany. [2]Liverpool School of Tropical Medicine, Pembroke Place, Liverpool L3 5QA, UK. [3]Institut de Recerca Biomèdica (IRB) and Institució Catalana de Recerca i Estudis Avançats (ICREA), Parc Cientific Barcelona, Josep Samitier 1-5, 08028 Barcelona, Spain. [4]CNRS UMR144, Institut Curie, Membrane and Cytoskeleton Dynamics Group, 26 Rue d'Ulm 75005 Paris, France. [5]Hybrigenics SA, 3-5 Impasse Reille, 75014 Paris, France. [6]Département de biochimie, Sciences II, 30, Quai Ernest Ansermet CH-1211 Genève 4, Switzerland.

*These authors contributed equally to this work
†Author for correspondence (e-mail: marcos.gonzalez@biochem.unige.ch)

Accepted 20 September 2007

The three main classes of trafficking factors implicated in cytokinesis are components of the secretory pathway, endocytic and/or recycling factors and membrane fusion machinery. Golgi proteins required for the secretory pathway such as Cog5 and Syntaxin5 are required for cytokinesis (Farkas et al., 2003; Xu et al., 2002). Endocytic recycling factors necessary for cytokinesis include Rab11 and Rab11FIP3/Arfophilin, which associate with the central spindle and furrow cortex (Skop et al., 2001; Wilson et al., 2005). Fusion machinery such as the exocyst complex and t- and v-SNAREs localizes at the mitotic midbody and furrow cortex, and is necessary for cytokinesis (Fielding et al., 2005; Finger et al., 1998; Gromley et al., 2005; Jantsch-Plunger and Glotzer, 1999; Low et al., 2003).

One membrane-trafficking component implicated in cytokinesis is the class III ADP ribosylation factor, ARF6. A constitutively active, GTPase-defective ARF6 mutant, ARF6Q67L, concentrated at the central spindle and midbody of HeLa cells, and ARF6Q67L overexpression caused late cytokinesis defects (Schweitzer and D'Souza-Schorey, 2002). Knockdown of ARF6 in HeLa cells using siRNA caused a late cytokinesis block (Schweitzer and D'Souza-Schorey, 2005). Possible effectors for ARF6 during cytokinesis are the Rab11/ARF6 binding proteins Rab11FIP3 and Rab11FIP4, which ARF6 recruits to the central spindle in HeLa cells (Fielding et al., 2005; Schweitzer and D'Souza-Schorey, 2002; Schweitzer and D'Souza-Schorey, 2005). ARF6 regulates endocytosis, recycling and actin remodelling (D'Souza-Schorey et al., 1995; Radhakrishna and Donaldson, 1997; Song et al., 1998). Via these mechanisms, ARF6 affects processes such as adherens junction disassembly and cell migration, including the formation of cord-like structures by hepatocytes in the mouse liver in response to hepatocyte growth factor (D'Souza-Schorey and Chavrier, 2006; Suzuki et al., 2006). In *Drosophila*, the ARF6-GEF Loner/Schizo is necessary for myoblast fusion (Chen et al., 2003) and midline crossing of axons (Onel et al., 2004).

In contrast to the central spindle microtubules and the actomyosin contractile ring, little is known about temporal and spatial coordination of membrane trafficking during cytokinesis. Many membrane-trafficking components are localized to the central

spindle (Skop et al., 2004), but the molecular machinery connecting the central spindle to membrane trafficking is unclear. Here we show that cytokinesis requires ARF6 in the *Drosophila* male germ line. ARF6 localizes to the plasma membrane and a population of early and recycling endosomes. In dividing cells, ARF6 is specifically enriched on recycling endosomes associated with the Pav central spindle. ARF6 is not required to target recycling endosomes to the central spindle, but is required for rapid membrane addition during cytokinesis. We suggest that ARF6 enrichment on recycling endosomes at the central spindle increases the rate of recycling to the plasma membrane, thus coordinating membrane recycling with the central spindle and cleavage furrow invagination during cytokinesis.

MATERIALS AND METHODS

Drosophila stocks

Imprecise excision of EP(2)2612 generated the deletions $arf6^{1}$, $arf6^{2}$ and $arf6^{3}$. Thirty nucleotides flanking sequence on each side of the deletions and the excision scar (italics) are shown, with asterisks indicating the boundaries of *arf6* sequence: $arf6^{1}$, TATACATGTGTATGTGTGTTACGGGCGT-GT**TCATGATGAAATA***ACGTACATAAATTACAAATGTTAAAAATG; $arf6^{2}$, TATACATGTGTATGTGTGTTACGGGCGTGT**TCATGATG-G***CGCGACGCCATCATACTGATATTTGCTAAC; $arf6^{3}$, TATACAT-GTGTATGTGTGTTACGGGCGTGT**TCATGACGCTCATGACG***TTAC-AACGATACCCACTGTGGGCTTTAATG. A linked lethal mutation in the *EP(2)2612* chromosome was cleaned by recombination. pav^{B200}, pav^{A375} and $chic^{13E}$ were previously described (Adams et al., 1998; Giansanti et al., 1998; Salzberg et al., 1994). Pav-GFP, GFP-α-tubulin, His2AvDGFP and DE-cad-GFP under polyubiquitin promoter control (Lee et al., 1988), and Sqh-GFP with the *sqh* promoter were previously described (Clarkson and Saint, 1999; Minestrini et al., 2003; Oda and Tsukita, 2001; Rebollo et al., 2004; Royou et al., 2004). γ-Tubulin GFP flies were a gift from S. Llamazares (IRB and ICREA, Barcelona, Spain).

Transgenics

Transgenic flies were generated by injecting the following vectors: P(Ubi:arf6-HA), a PCR product containing ARF6 coding sequence from the LD22876 clone (BDGP EST Project) with *Sac*I and *Xba*I sites in primer overhangs and including a C-terminal HA epitope tag was cloned between *Sac*I and *Xba*I sites of pSRalpha. A *Sac*I-*Xba*I fragment excised from PSRalpha was ligated between *Sac*I and *Xba*I sites of TOPO. A *Kpn*I-*Xba*I fragment from the resulting vector was cloned between the polyubiquitin vector *Kpn*I and *Spe*I sites. P(w^{+}arf6^{+}) *arf6* rescue construct, a 3.8 kb PCR product from genomic DNA containing *arf6* and flanking sequences was cloned into TOPO-XL. The 3.8 kb fragment from *Xba*I, *Not*I and *Sph*I digestion was inserted between *Not*I and *Xba*I sites of pCasper4. P(UbiGFP-Rab5) and P(UbiGFP-Rab11) were generated from pUAST-GFP-Rab5 (Wucherpfennig et al., 2003), and pUAST-GFP-Rab11 (Emery et al., 2005). P(UbiGFP-Rab4), PCR product containing *rab4*-coding sequence from pOT2-GH18176 with primer overhang *Xho*I-sites was cloned into the *Xho*I site of pEGFP-C3. The *Nhe*I-*Xba*I fragment from pEGFP-C3-rab4 was inserted in the pUAST *Xba*I-site. In all cases, GFP-Rab containing *Not*I-*Xba*I fragments from pUAST were cloned between polyubiquitin vector *Not*I and *Xba*I sites.

Antibodies and microscopy

A rabbit polyclonal antibody generated (Eurogentec) against amino acids 99-112 of *Drosophila* ARF6 (ARTELHRIINDREM) binds ARF6 at 20 kDa in western blots. Rabbit anti actin (Sigma A2066) was used 1:400. Anti-ARF6 was used 1:50 for western blotting, but was unsuitable for immunofluorescence.

Embryo immunofluorescence staining was performed using standard techniques. Mouse antibody BP102 (Hybridoma Bank) was used 1:30, and Rabbit anti MHC (Kiehart and Feghali, 1986) at 1:500. *arf6* embryos zygotically rescued by *CyO, hb-lacZ* were identified using rabbit anti β-galactosidase (Cappel) 1:500. Testes dissected in PBS were fixed for 20 minutes in PBS containing 4% paraformaldehyde, and a further 20 minutes after the addition of 0.2% Triton X-100. After washing with PBS, subsequent staining and washing steps were performed in PBS containing 0.1% Triton X-100. A 2-hour block with 0.5% BSA was followed by overnight incubation at 4°C with 0.5% BSA and primary antibodies: rat anti-HA (clone 3F10, Roche), 1:500, rabbit anti-Pav 1:250 (Adams et al., 1998). After three 20-minute washes, primary antibodies were detected using Alexa Fluor 546-conjugated anti-rat (Molecular Probes) and Cy5-conjugated anti-rabbit (Jackson ImmunoResearch Laboratories) antibodies at 1:500, with 2% normal goat serum for 2 hours at room temperature.

Confocal images were acquired using Zeiss LSM 510 and LeicaDMIRE2, TCS SP2 SP2 microscopes, with 63× (NA 1.4) and 100× (NA 1.4) objective lenses. Colocalization (± s.e.m.) was quantified in unprocessed images in the Zeiss LSM image browser by manually counting punctae. In dividing cells, punctae within 3 μm of Pav staining were classified as 'central spindle' localized, other punctae as 'non central spindle'. Images were processed for contrast/brightness, levels and 'dust and scratches' with Adobe Photoshop 7.0 (Adobe Systems).

Live imaging

Spermatocyte imaging was carried out as described (Rebollo and Gonzalez, 2004). Cell perimeter and diameter were measured in ImageJ (http://rsb.info.nih.gov/ij/). Furrow ingression, perimeter and surface area rates are linear regression line slopes. Four to six confocal sections were maximally projected, except Sqh-GFP.

Germ line clones of *arf6* mutants

Germline clones were generated using the flp/FRT systems described (Chou and Perrimon, 1992). Females (genotype *y w hsflp;* $FRTG13Ovo^{D1}/FRTG13arf6^{1}$) raised at 25°C were heat shocked for 2 hours at 38°C as third instar larvae to activate the flippase, generating germ line clones (genotype *y w hsflp;* $FRTG13arf6^{1}/FRTG13arf6^{1}$). *y w hsflp;* $FRTG13Ovo^{D1}/FRTG13arf6^{1}$ females were crossed for 3 days to wild-type males in vials supplemented with fresh yeast before collecting eggs. The same procedure was used for $arf6^{3}$.

Yeast two-hybrid analysis

PCR from clone LD22876 generated a Glu67-Leu substitution of the ARF6 ORF. *Not*I and *Spe*I overhang sites were generated by PCR and the resulting fragment cloned into pB27 bait plasmid derived from pBTM116 (Vojtek and Hollenberg, 1995). A random-primed cDNA library from 0-24 hour *Drosophila* embryo poly(A^{+}) RNA was constructed into the pP6 plasmid derived from pGADGH (Bartel et al., 1993). The two-hybrid system was used to detect protein-protein interactions (Bartel, 1993). The library was transformed into the Y187 yeast strain. Around 10 million independent yeast colonies were collected, pooled and stored at –80°C, and over 50 million interactions tested using a previously described mating protocol (Fromont-Racine et al., 1997). Prey fragments of positive clones were PCR amplified and sequenced at 5′ and 3′ junctions. Corresponding genes were identified in the GenBank database (NCBI) using an automated procedure (Formstecher et al., 2005).

Pav-binding assay

DNA encoding Pav655-865 was cloned into pGEX4T1 at the GST C-terminus. pGEX4T1Pav655-865 and pGEX4T1 were transformed into *E. coli* strain B21, and expression induced by 1 mM isopropyl β-D-thiogalactopyranoside for 5 hours at 20°C. GST proteins were affinity purified using glutathione-Sepharose beads (Amersham Biosciences), eluted using glutathione, dialyzed against 20 mM Tris-HCl, pH 7.4, 150 mM NaCl, 2 mM EDTA, 2 mM β-mercaptoethanol and 10% glycerol, and stored at –80°C. HeLa cells were transfected with pSRalpha(ARF6HA) and pSRalpha(ARF6Q67LHA) using Effectene (Qiagen), lysed after 20-24 hours in 50 mM Tris-HCl pH 5.5, 137 mM NaCl, 1% Triton X-100, 10 mM $MgCl_2$, 10% glycerol (Buffer B) with complete protease inhibitor cocktail tablets (Roche), and centrifuged for 15 minutes at 13,000 rpm (15,000 ***g***) at 4°C. Supernatants were incubated with 20 μg of GST fusion protein for 15 minutes at 4°C with 0.5% BSA, and for 1-2 hours at 4°C after adding glutathione-Sepharose beads. Beads were washed three times in Buffer B, once in Buffer B containing 0.1% SDS and once in PBS. Bound proteins were eluted using 4× NuPage LDS sample buffer (Invitrogen) and assayed

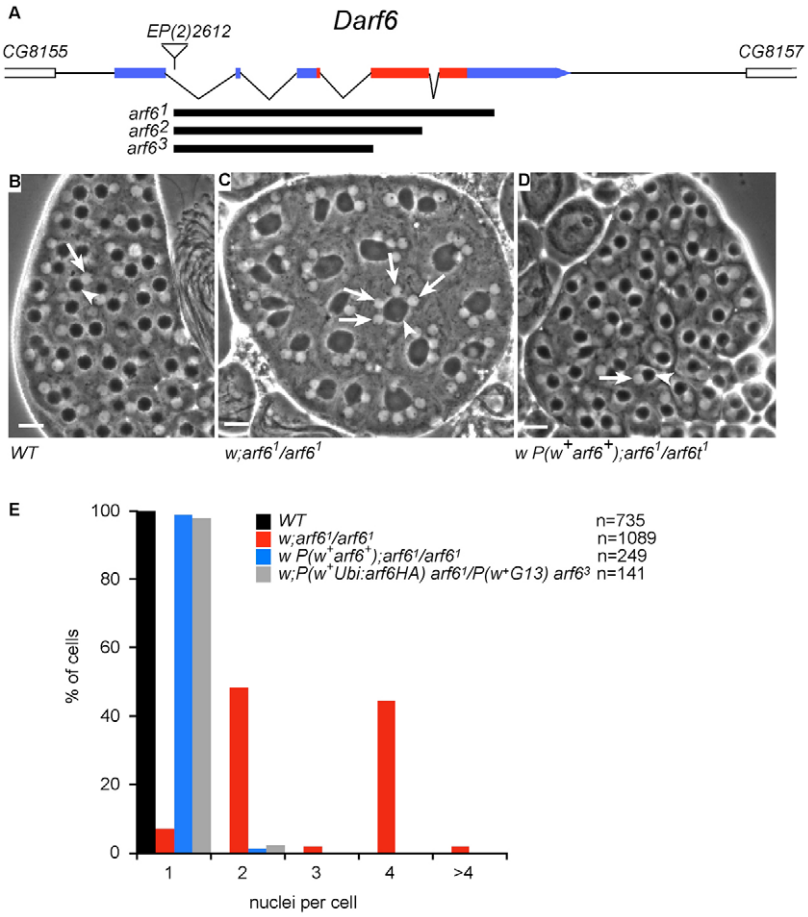

Fig. 1. *Drosophila* ARF6 is required for cytokinesis in testes. (**A**) The portion of genomic region 51f encoding *Drosophila* ARF6 (blue), and protein coding sequences of *arf6* (red). *arf6*^{1}, *arf6*^{2} and *arf6*^{3} (below) are deletions produced by imprecise excision of EP(2)2612. (**B-D**) Phase-contrast images of spermatids after the second meiotic division, showing white nuclei (arrows) and black mitochondrial derivatives (*Nebenkerne*, arrowheads). (B) WT, (C) *arf6*^{1} homozygotes: two or four nuclei per cell. (D) A rescue construct expressing *arf6* from the endogenous promoter restores a 1:1 ratio of nucleus to *Nebenkern* per cell. Scale bars: 20 μm. (**E**) Frequency of nuclei per cell in WT, *arf6*^{1}, *arf6*^{1} rescued by the *arf6* endogenous rescue construct and *arf6*^{3} rescued by expression of ARF6HA. *n,* number of cells counted.

by western blotting with rabbit anti-HA antibody at 1:500 (Roche) and affinity-purified polyclonal rabbit anti-GST at 1:10,000 (Protein Expression and Purification Facility, MPI-CBG, Dresden).

Perimeter and surface area measurement

To test the suitability of perimeter as a measure of surface area, six control cells were cultured with 8 μM FM4-64 (Molecular Probes) in Schneider's medium with 10% fetal calf serum. In these conditions spermatocytes are almost rotationally symmetrical. The cell outline of the mid confocal plane of non-tilted cells was used to calculate surface area capitalizing on this rotational symmetry, approximating the cell by a series of around 20 cone segments. Software used to calculate the surface area from cell outlines available upon request (pdfoster@ntlworld.com). For each cell, perimeter was roughly linearly related to surface area:

$$P = mS + c \ ,$$

where P is perimeter; S, surface area; m, slope of the linear regression line; and c, intercept on the perimeter axis. The value of m was similar for different cells, whereas c was more variable (see Fig. S4C, Table S2 in the supplementary material). Therefore, without making a complete set of measurements on a cell, it is difficult to infer the surface area from the perimeter. However, the rate of perimeter change indicates of the rate of surface area change well.

Let P_1 be the perimeter, and S_1 the surface area at time t_1, and P_2 be the perimeter and S_2 the surface area at time t_2.The perimeter change between t_1 and t_2 is:

$$P_2 - P_1 = (mS_2 + c) - (mS_1 + c) = m(S_2 - S_1) \ .$$

Therefore the rate of perimeter change for time period t_1 to t_2 is:

$$(P_2 - P_1)/\ (t_2 - t_1) = m(S_2 - S_1)/\ (t_2 - t_1) \ .$$

Therefore, rate of perimeter change can be used to indicate surface area rate change, since the cell-specific c term is eliminated: only the slope of the relationship between surface area and perimeter is relevant.

Cell volume was calculated as the product of the cell area in each slice and the slice separation, from stacks of optical slices taken at 0.51 μm intervals through spermatocytes expressing DE-cad-GFP.

RESULTS

Drosophila arf6 is a non-essential gene required during spermatogenesis

To study ARF6-dependent endocytic trafficking, we generated deletions in the *arf6* gene by imprecise excision of the EP(2)2612 transposable element in intron 1 (Fig. 1A). A null mutation, *arf6*^{1}, corresponding to a 1709-nucleotide deletion in the transcribed region, entirely removed the ORF (Fig. 1A). Consistently, an antibody against *Drosophila* ARF6 detected no ARF6 protein in western blots from homozygous *arf6*^{1} flies (see Fig. S1A in the supplementary material).

ARF6 is not essential for fly viability. Homozygous *arf6*^{1} progeny from homozygous mutant mothers (maternal/zygotic mutants) were viable until adulthood, presenting no overt external morphological phenotype. Recent reports show that expression of a GDP-bound dominant negative ARF6 protein (ARF6TN) impairs myoblast fusion and axon path finding during embryogenesis (Chen et al., 2003; Onel et al., 2004). Both developmental events occurred normally in *arf6* null mutant embryos (see Fig. S1B-E in the supplementary material), indicating that the ARF6TN protein causes secondary defects beyond the suppression of ARF6 function.

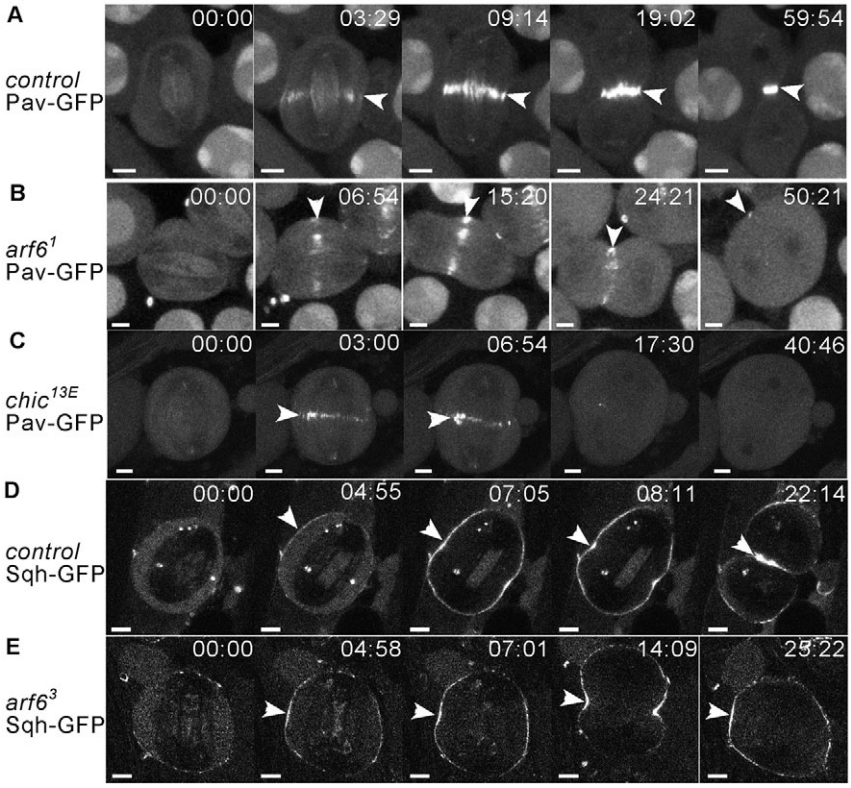

Fig. 2. ARF6 is not required for central spindle or contractile ring formation. (**A-E**) Time-lapse images of Pav-GFP (A-C) and Sqh-GFP (D,E) during cytokinesis in control (A,D), *arf6* (B,E) and *chic*^{13E} mutant spermatocytes (C). Times are minutes:seconds after anaphase onset (min AA). Scale bars: 5 μm. (A) Control, Pav-GFP accumulates at the central spindle during anaphase B (arrowhead, 03:29). Central spindle microtubules labelled with Pav-GFP bundle and compact into a dense midbody (arrowheads, 09:14-59:54). (B) *arf6*^{1}, anaphase B Pav-GFP central spindle accumulation occurs (arrowhead, 06:54). Pav-GFP-labelled microtubules bundle (arrowhead, 15:20), a cleavage furrow initiates, but central spindle Pav-GFP signal declines (arrowhead, 24:21). After furrow regression, only a tiny amount of Pav-GFP remains at the cortex (arrowhead 50:21). (C) *chic*^{13E}, anaphase B Pav-GFP central spindle accumulation occurs (arrowhead, 03:00, 06:54), but no furrow is initiated. 17:30 min AA: very little Pav-GFP remains at the central spindle. (D) Control, Sqh-GFP transfers to the cortex (arrowhead, 04:55), accumulates at the future cleavage furrow site (arrowheads, 07:05, 08:11) which then invaginates (arrowhead, 22:14). (E) *arf6*^{3}, Sqh-GFP transfers to the cortex (arrowhead, 04:58) concentrating at the future cleavage furrow site (arrowheads 07:01, 14:09). Sqh-GFP remains at the cortex during and after regression (arrowhead, 25:22). Genotypes: *w; arf6*^{1}*/CyO; Pav-GFP/TM6B* (A), *w; arf6*^{1}*/ arf6*^{1}*; Pav-GFP/TM6B* (B), *chic*^{13E}*/chic*^{13E}*; Pav-GFP/TM6B* (C), *y w sqh*^{AX3}*; +; P (w+ sqh-gfp)* (D), *y w sqh*^{AX3}*; arf6*^{3}*/arf6*^{3}*; P (w+ sqh-gfp)* (E).

Female *arf6*^{1} flies showed reduced fertility because of a partially penetrant requirement for ARF6 during chorion formation in the germ-line (see Fig. S2 and Table S1 in the supplementary material). Male *arf6*^{1} flies were completely sterile. Mutant spermatids showed a 'four-wheel-drive' phenotype, indicating a cytokinesis defect during spermatocyte meiosis (Fuller, 1993) (Fig. 1B-E): over 90% of spermatids contained more than one nucleus, and 41% had four nuclei per mitochondrial *Nebenkern* derivative (Fig. 1E), corresponding to 79% failure in cytokinesis during the two meiotic divisions (see Fig. S3 in the supplementary material). 1.9% of cells showed 8:1 nuclei-to-*Nebenkern* ratios, suggesting that cytokinesis of gonial cell mitosis prior to meiosis is also occasionally affected, as previously suggested for other cytokinesis mutants (Brill et al., 2000; Giansanti et al., 2004). *arf6*^{2} and *arf6*^{3} showed phenotypes indistinguishable from *arf6*^{1}. Male sterility and the mutant cytokinesis phenotype are due to the *arf6*^{1} mutation, because an *arf6*$^{+}$ genomic transgene rescued the defects, yielding fertile males (Fig. 1D,E).

ARF6 is required for cleavage furrow progression

Videomicroscopy of control and mutant cells during meiosis I was performed to characterize the cytokinesis defect. *arf6* mutant spermatocytes expressing Histone2A-GFP and γ-Tubulin GFP showed that chromosome segregation and centrosome behavior occurs normally (not shown). α-Tubulin GFP fusion (GFP–α-tubulin) indicated that spindle initially forms normally in *arf6*^{1} mutant spermatocytes (see Movies 1, 2 in the supplementary material). In *arf6* mutant cells, a cleavage furrow was established, but later regressed. We therefore analyzed furrow ingression kinetics in wild-type and *arf6* mutant spermatocytes.

In control cells, cell shape and diameter were constant until anaphase onset (see Fig. 4B and Movies 1, 3, 4, 7 and 9 in the supplementary material). After anaphase onset, cells elongated, decreasing in equatorial diameter at 0.4 μm/minute (Fig. 3B, Fig. 4C). During anaphase B, which starts 2 minutes after anaphase onset (min AA), Pav accumulated at the central spindle (Minestrini et al., 2003) (Fig. 2A, Fig. 3A, Fig. 4C; see Movie 3 in the supplementary material). The centralspindlin complex subsequently signals to the cortex, and the actomyosin contractile ring forms. Myosin regulatory light chain (Sqh-GFP) accumulated at the future cleavage furrow 1 minute after the onset of Pav accumulation at the central spindle (Fig. 2D, Fig. 3A; see Movie 4 in the supplementary material) (Adams et al., 1998; Royou et al., 2004; Somers and Saint, 2003). Shortly after Pav and Sqh accumulation, equator contraction accelerated to

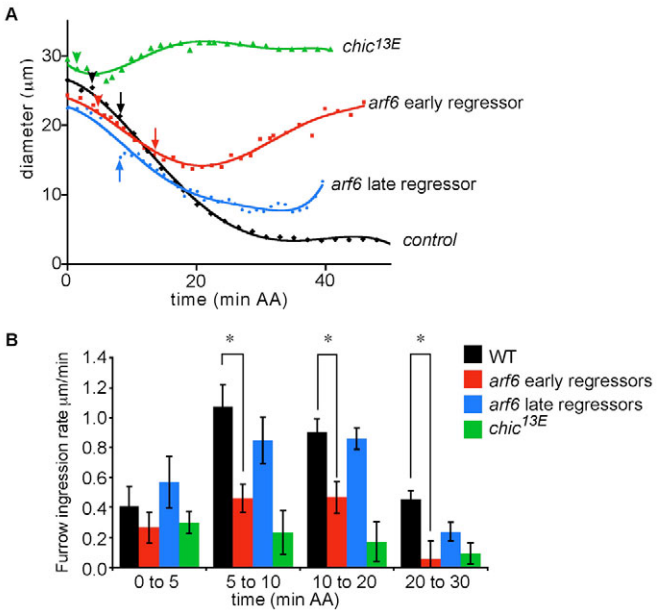

Fig. 3. ARF6 is required for rapid cleavage furrow invagination. (**A**) Representative results for control, *arf6* mutant 'early regressor', 'late regressor' and *chic*^{13E} illustrate furrow progression, timing of Pavarotti concentration at central spindle (arrowheads) and indented cleavage furrow appearance (arrows). Diameter is measured at furrow tip or future furrow site. (**B**) Furrow ingression rates in control (black), *arf6* late regressors (blue) *chic*^{13E} (green) and *arf6* early regressors (red). Furrow ingression is significantly impaired in *arf6* mutants compared with control cells: **P*<0.01, Student's *t*-test. min AA, minutes after anaphase onset.

1 μm/minute (Fig. 3, Fig. 4C). Five minutes after Pav accumulation, a plasma membrane indentation, the 'cleavage furrow', appeared (Fig. 2A, Fig. 3A, Fig. 4C). The furrow progressed at 1 μm/minute, finally decelerating to stop around 35 minutes after anaphase onset at width 3-5 μm (Fig. 2A, Fig. 3A, Fig. 4C; see Fig. S4A in the the supplementary material). This narrow opening between the two daughter cells differentiates into the ring canal (Hime et al., 1996).

In time-lapse movies, cytokinesis failed in 89% of *arf6*^{1} cells, consistent with the frequency of multinucleated spermatids (see Fig. S3B in the supplementary material). Cytokinesis failed early during furrow progression in 55% of the failing cells. The remaining 45% of failing cells were 'late regressors', in which cytokinesis proceeds with normal kinetics of furrow formation and progression until the furrow is less than 10 μm wide. The furrow stays at this diameter for a variable time period before collapsing (Fig. 3A; see Fig. S4A in the supplementary material). During furrow progression, plasma membrane was also added with normal kinetics (see below; Fig. 4B; see Fig. S4B in the supplementary material).

In 'early regressors', anaphase B-cell elongation occurred. The equator contracted at 0.3 μm/minute, only slightly slower than in the wild type (Fig. 3B, Fig. 4C). Pav and Sqh central spindle and contractile ring targeting occurred only slightly later than in the wild type (Fig. 2B,E, Fig. 4C; see Movies 5 and 6 in supplementary material). However, fast equator contraction did not occur, only accelerating to 0.5 μm/minute, and indentation occurred 10 minutes, instead of 5 minutes after central spindle Pav accumulation (Fig. 2B, Fig. 3A, Fig. 4C). Shortly after the cleavage furrow indentation appeared, when it is around 15 μm wide, the furrow regresses. After cleavage furrow collapse, Pav dissociates from the central spindle, although Sqh remains at the cortex during regression (Fig. 2E; see Movie 6 in the supplementary material).

These observations indicate that ARF6 is not necessary for targeting Pav to the central spindle, or for actomyosin ring formation. The mutant phenotypes reveal two critical phases for ARF6 function during cytokinesis: (1) an early role during cleavage furrow progression after furrow initiation, and (2) a later role in ring canal establishment at the end of cytokinesis. Since ring canal stabilization may be a specialized event restricted to germ cells, and may be due to the higher frequency of the early regressors, we decided to concentrate on the early regressors and the early role of ARF6 in furrow progression.

ARF6 is required for rapid plasma membrane addition during cytokinetic cleavage furrow progression

Spermatocytes divide, producing two daughter cells with half the volume of the mother (volume change 0.8±1.4%, *n*=5 cells). For spherical cells, this implies that the membrane surface increases by 26% during cytokinesis. We therefore investigated whether the *arf6* phenotype is caused by a defect in membrane addition to the cell surface. The absence of surface increase could lead to an increase in membrane tension, which would counteract the forces generated by the contractile ring. This hypothesis was prompted by the established role of ARF6 during endocytic membrane recycling (D'Souza-Schorey et al., 1998; Prigent et al., 2003; Radhakrishna and Donaldson, 1997) which might be essential for rapid membrane addition from an endosomal, ARF6-dependent membrane store.

The kinetics of plasma membrane increase during meiosis I was studied by measuring cell perimeter of spermatocytes in confocal images, as well as the total surface area calculated for 3D-reconstructed cells (Fig. 4; see Fig. S4 in the supplementary material). Experiments on the relationship between perimeter and surface area changes indicated that perimeter increase correlates well with surface area increase (see Fig. S4C in the supplementary material). Plasma membrane growth during meiosis I was negligible prior to anaphase. Membrane increase started during anaphase B cell elongation at 0.6 μm/minute. This 'perimeter rate' corresponds to a membrane addition of around 8 μm^2/minute (see models in the supplementary material). The perimeter rate increased greatly (2.5-fold, corresponding to around 22 μm^2/minute) directly after the onset of Pav accumulation, peaking around 15 min AA at the time of maximum furrow ingression rate and the appearance of membrane indentation (Fig. 4B,C). Subsequently, the rate decreased until the completion of cytokinesis. In *arf6* mutants, slow membrane addition characteristic of early cytokinesis was maintained after furrow membrane indentation, and the rapid membrane addition phase never occurred (Fig. 4B,C; see Fig. S4B in the supplementary material). These data suggest that ARF6 is involved in rapid membrane addition to the plasma membrane, which is necessary during the rapid contraction of the actin ring during cytokinesis.

Membrane addition to the plasma membrane is uncoupled from actomyosin ring contraction

The *arf6* mutant phenotype reveals a link between cleavage furrow progression and rapid membrane surface increase. To find out whether cleavage furrow progression defects lead to a defect in surface increase, or vice versa, we studied furrow progression and membrane addition rates in profilin *chickadee* (*chic*) mutants (Cooley et al., 1992; Giansanti et al., 1998). In *chic*^{13E} mutants, the

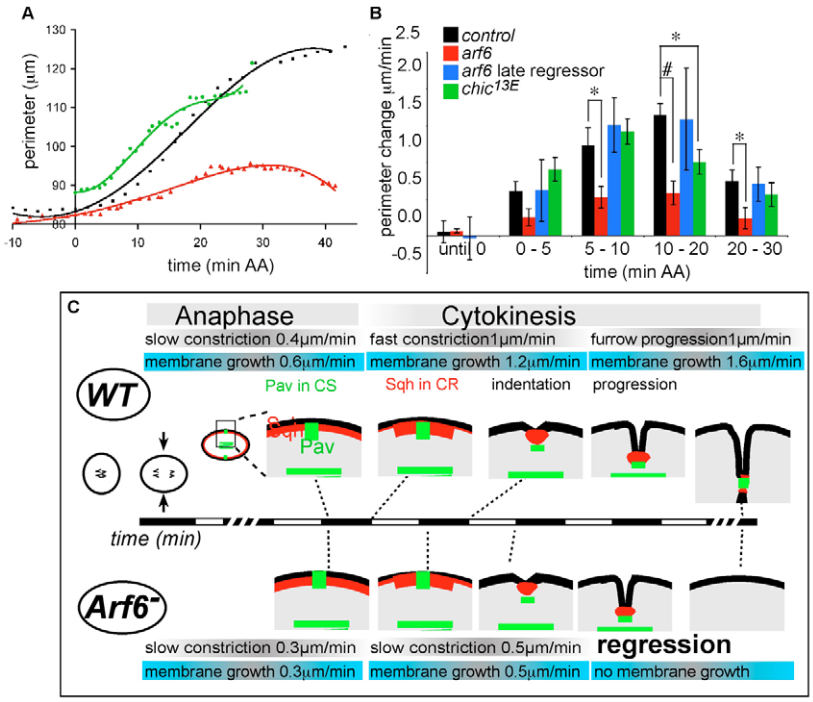

Fig. 4. ARF6 is required for rapid growth of the plasma membrane during cytokinesis. (**A**) Representative cells for control, *arf6* early regressor and *chic*^{13E} cells illustrate perimeter kinetics during anaphase and cytokinesis. (**B**) Rate of perimeter change in control, *arf6* early and late regressors, and *chic*^{13E} cells. Membrane insertion is significantly impaired in *arf6* from 5 min AA onwards: $*P<0.05$ and $^{\#}P<0.001$, Student's *t*-test. Membrane insertion is not significantly impaired in *chic*^{13E} mutants until central spindle disassembly (cf. 5-10 min AA with 10-20 min AA). Error bars represent s.e.m. (**C**) Timeline of the events of cytokinesis and the rates of cytokinesis furrow ingression and perimeter change (membrane growth) in control and *arf6* early regressors, with respect to central spindle Pav-GFP appearance. Black and white bars represent 1-minute intervals. CS, central spindle; CR, contractile ring.

central spindle initially formed normally and Pav was targeted properly (Fig. 2C), but actomyosin contractile ring formation fails (Giansanti et al., 1998). As a consequence, furrow ingression kinetics are even more affected than in *arf6* mutants (Fig. 3). However, in these *chic*^{13E} cells, membrane addition initially occurred with kinetics similar to control cells, until the premature disassembly of the central spindle and Pav-GFP disappearance from the central spindle area (Fig. 2C, Fig. 4A,B; see Fig. S4B in the supplementary material).

These results imply that the actomyosin ring contraction and cleavage furrow progression are not essential for the rapid membrane-addition phase. Lack of rapid membrane addition is a specific feature of the *arf6* mutants, not a trivial consequence of furrow ingression failure. The data leave open a possible role for the Pav central spindle during the process.

ARF6 endosomes are associated with the Pav central spindle during cytokinesis

We then studied the subcellular localization of ARF6, its possible association with intracellular endosomal membranes, and the Pav central spindle. We used GFP-Rab4 as a marker for early endosomes along the fast recycling route to the plasma membrane, and GFP-Rab11 to label recycling endosomes along the kinetically slower recycling route (Sheff et al., 1999; van der Sluijs et al., 1992). Functional HA-tagged ARF6 was expressed from the polyubiquitin promoter. This expression rescued the *arf6* mutant cytokinesis and chorion phenotypes (Fig. 1E; see Fig. S2D in the supplementary material). ARF6-HA was present in the cytosol and enriched at endosomes and the plasma membrane, as previously reported in mammalian cells (Fig. 5; see Fig. S5 in the supplementary material) (D'Souza-Schorey and Chavrier, 2006).

The results of the localization analysis are summarized in Table 1. Early during meiosis I cytokinesis, ARF6-positive endosomes (66% of punctae) associated with Pav-positive central spindle microtubules including the cortical microtubule population where the cleavage furrow forms (Table 1, Fig. 5A-B,D, arrowheads; see Fig. S5D in the supplementary material). This contrasts with 52% of Rab4 endosomes and 40% of Rab5 endosomes associated with the central spindle during meiosis I (Table 1). The ARF6 central spindle endosomal population corresponds mainly (87%) to Rab4-labelled endosomes.

Rab11 recycling endosomes are also recruited to the central spindle and decorated with ARF6 (Table 1, Fig. 5B). Unlike ARF6/Rab4 endosomes, Rab11/ARF6 endosomes are only enriched at the central spindle late in cytokinesis when the cleavage furrow is almost fully ingressed [4.9±0.4 μm across (mean ± s.e.m.), n=11 cells]. This suggests that both Rab4 and Rab11 recycling endosomes participate in plasma membrane addition during cytokinesis. However, the late appearance of Rab11 endosomes at the central spindle in control cells, at a time when the furrow had already collapsed in *arf6* early regressors, instead suggests a role for Rab11 ring canal stabilization, which might be critically affected in the *arf6* 'late regressors'.

In summary, recycling endosomes at the central spindle contain ARF6. Is ARF6 specifically enriched in the central spindle population of Rab4 and Rab11 recycling endosomes? Most central spindle Rab4 endosomes (73%) were decorated by ARF6 whereas only 22% of the Rab4 endosomes not localized to the central spindle contained ARF6 (Table 1, Fig. 5C). Similarly, 85% of Rab11 endosomes at late central spindles contained ARF6, versus 10% elsewhere in the cell (Table 1, Fig. 5C). These data indicate that ARF6 targeting to recycling endosomes is specifically biased towards the central spindle endosomal population.

Since central spindle recycling endosomes are enriched in ARF6, we asked whether ARF6 itself targets recycling endosomes to the central spindle. We therefore observed Rab4 and Rab11 endosome distribution in time-lapse movies. In *arf6*^{1} mutants, rab4 endosomes were targeted to the central spindle as in wild-type controls (Fig. 6A,B; see Movies 7 and 8 in the supplementary material). Therefore, ARF6 does not target endosomes to the spindle, but instead functions downstream of endosomal targeting. ARF6 does not seem

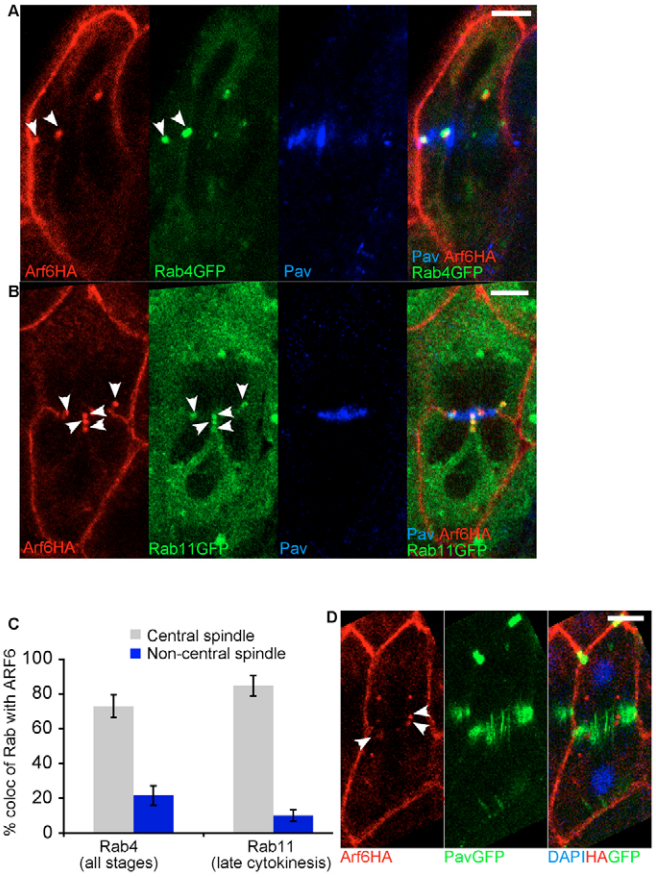

Fig. 5. ARF6 endosomes at the Pav central spindle during cytokinesis. (**A,B**) Fixed primary spermatocytes. (A,B) ARF6HA (red) and Pav (blue) immunostaining and Rab-GFP [green; Rab4 (A) and Rab11 (B)]. ARF6HA colocalizes with GFP-Rab4 (A) and GFP-Rab11 (B) at the central spindle (arrowheads). (**C**) Colocalization frequency of GFP-Rab4 (n=17 cells) and GFP-Rab11 (n=13 cells) with ARF6HA at the central spindle during cytokinesis (grey) or elsewhere in the cell (blue). Error bars represent s.e.m. (**D**) Primary spermatocyte initiating furrow. ARF6HA (red) is already partially localized to the central spindle (arrowheads), labelled with Pav-GFP (green). DAPI labels chromosomes (blue). Scale bars: 5 μm.

to play a direct role in Rab11 targeting either. In the *arf6* late regressors, the regression occurred around the time when Rab11 accumulation was clearly observed. However, we observed *arf6* late regressors in which Rab11 endosome localization does not appear to be affected (Fig. 6C,D; see Movies 9 and 10 in the supplementary material).

In summary: (1) Rab4 and Rab11 recycling endosomes are targeted to the central spindle; (2) ARF6 targeting is biased towards the central spindle population of recycling endosomes; but (3) ARF6 does not target recycling endosomes to the central spindle. Instead, another machinery must target ARF6 to central spindle endosomes. ARF6 could then endow the endosomal membrane stores with rapid recycling kinetics necessary for rapid membrane addition during fast cleavage furrow progression.

ARF6 binds the centralspindlin component Pavarotti

What targets ARF6 to central spindle endosomes? Using a *Drosophila* embryo cDNA library, Pav was identified in a two-hybrid screen for proteins interacting with *Drosophila* ARF6Q67L mutant (Fig. 7A). Five clones corresponding to the Pav ORF define the ARF6-binding domain: a region adjacent to the coiled-coil domain of Pav (amino acids 727-844; Fig. 7B). Binding assays confirmed this interaction (Fig. 7C). These results suggest that Pav might contribute to ARF6 recruitment to central spindle endosomes.

DISCUSSION

Dividing a sphere into two spheres that sum up to the same volume requires a net surface area increase of 26%. During meiosis I cytokinesis in *Drosophila* spermatocytes, 500 μm^2 of plasma membrane are added in around 20 minutes, posing a logistical problem of adding plasma membrane at an average rate of over 0.4 μm^2/second. In this report, we have shown that ARF6 helps to solve this problem by mediating the rapid mobilization of endocytic membrane stores in recycling endosomes at the central spindle. This is supported by two lines of evidence: (1) In *arf6* null mutants, cytokinesis failed in 80% meiotic divisions (Fig. 1; see Fig. S3 in the supplementary material) owing to a defect in rapid plasma membrane addition (Fig. 4; see Fig. S4 in the supplementary material) ultimately causing furrow regression (Fig. 3; see Fig. S4 in the supplementary material); and (2) Rab4 and Rab11 endosomes at the central spindle are enriched in ARF6 (Fig. 5). Without ARF6, recycling endosomes are still targeted to the central spindle, but membrane insertion is slow. These data suggest that ARF6 modifies the membrane dynamics of recycling endosomes to achieve a high recycling rate. The results pose the following questions: why are recycling endosomes targeted to the central spindle? How does ARF6 modify the membrane dynamics? Why are there *arf6* early and late regressors? Why is ARF6 only required for male meiosis? We discuss these four issues below.

Plasma membrane addition during cytokinesis: secretory versus endocytic trafficking

Four solutions exist to the demand for rapid surface area increase during cytokinesis: (1) decreasing cell volume; (2) stretching existing membrane; (3) resolving membrane microvilli; and (4)

Table 1. Colocalization statistics of ARF6 with Rabs at endosomes

	ARF6*	Rab4*	Rab5*	Rab11†
Punctae at central spindle	66±4 (n=41)	52±6 (n=17)	40±5 (n=10)	42±8 (n=13)
Colocalising with ARF6 (central spindle)		73±7 (n=17)	ND	84±6 (n=13)
Colocalising with ARF6 (not central spindle)		22±5 (n=17)	ND	10±4 (n=13)
Colocalising with Rab4 (central spindle)	87±5 (n=17)		ND	ND
Colocalising with Rab4 (not central spindle)	56±11 (n=17)		ND	ND
Colocalising with Rab11 (central spindle)	37±11 (n=12)	ND	ND	
Colocalising with Rab11 (not central spindle)	43±8 (n=12)	ND	ND	

Data are presented as % of punctae ± s.e.m.; n, number of cells quantified; ND, not determined.
*Cells in all stages of cytokinesis after initiation of cleavage furrow invagination.
†Only cells in late cytokinesis (maximum diameter at cleavage furrow 13.5 μm).

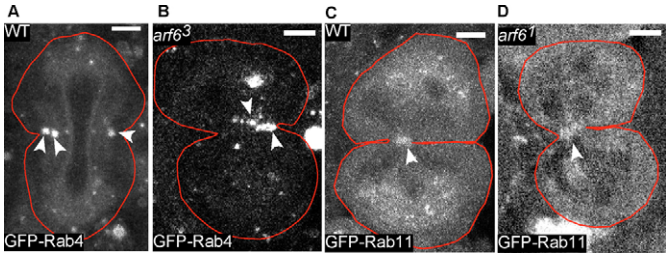

Fig. 6. ARF6 is not required for the localization of recycling endosomes to the central spindle. (**A-D**) Live primary spermatocytes in meiosis I, expressing GFP-Rab4 (A,B) or GFP-Rab11 (C,D) in control (A,C) and *arf6* early (B) or late regressor cells (D). Arrowheads, GFP-Rab4 and GFP-Rab11 at the central spindle in control and *arf6* mutants. Red, cell outlines determined by DIC. Scale bars: 5 μm.

delivering membrane to the surface. There are no reports of cell volume decrease during cytokinesis. Under tension, the surface of biological membranes stretches by only 2-3% before lysis, (Needham and Hochmuth, 1989). In P815Y mastoma cells, unfolding of microvilli accumulated during interphase is sufficient to account for the surface area increase during cytokinesis (Knutton et al., 1975). By contrast, microvilli in some ascidian eggs show the converse behavior, increasing in number during cleavage furrow progression and disappearing during interphase, suggesting that this mechanism is not conserved (Satoh and Deno, 1984). Cells that do not produce sufficient extra surface area between G1 and cytokinesis, must increase membrane surface during cytokinesis by delivering membrane to the surface.

Two trafficking systems control membrane addition to the plasma membrane: the secretory pathway (ER-to-Golgi-to-plasma membrane) and the endocytic pathway (recycling-endosome-to-plasma membrane). Golgi-to-endosome traffic represents a mix of these two pathways (Ang et al., 2004). Both secretory and endocytic factors are implicated in cytokinesis (Echard et al., 2004; Eggert et al., 2004; Skop et al., 2004). The relative contribution of the endocytic versus the secretory pathway to cytokinesis may depend on the rate of membrane deposition that the pathway can deliver, relative to the speed of cytokinesis. Meiosis I cytokinesis in *Drosophila* spermatocytes is very demanding, requiring 500 μm^2 expansion in 20 minutes. Endocytic recycling can make large stores of membrane available rapidly without de novo synthesis (Pelissier et al., 2003). Indeed, in BSC1 cells, endocytic recycling, but not the addition of newly synthesised membrane from the Golgi, is sufficient for the increase in plasma membrane surface during cytokinesis (Boucrot and Kirchhausen, 2007).

The analysis of membrane addition kinetics in wild-type and *arf6* cells reveals two components of membrane addition: a slow ARF6-independent process and, after central spindle formation, a 2.5-fold faster addition process boosted by ARF6 (Fig. 4). The accelerated addition rate coincides with the positioning of Rab4/ARF6 endosomes at the cleavage furrow early during cytokinesis. Rab11/ARF6 recycling endosomes might be involved later for stabilization of the ring canals. The slow component might correspond to secretory trafficking, or other ARF6-independent recycling routes. Indeed, in addition to ARF6, Golgi factors such as Cog5 and Syntaxin 5 have been implicated in the process of cytokinesis in *Drosophila* testes (Farkas et al., 2003; Xu et al., 2002). It will be interesting to see the rate effects of mutants of these factors in comparison to *arf6*.

Why are some *arf6* mutant cells impaired in the rate of plasma membrane addition causing early regression of the cleavage furrow, whereas other cells show a normal addition rates and only a late regression phenotype? We favor the possibility that the lack of ARF6 uncovers a natural variation in the activities of other components involved in plasma membrane insertion, or in the

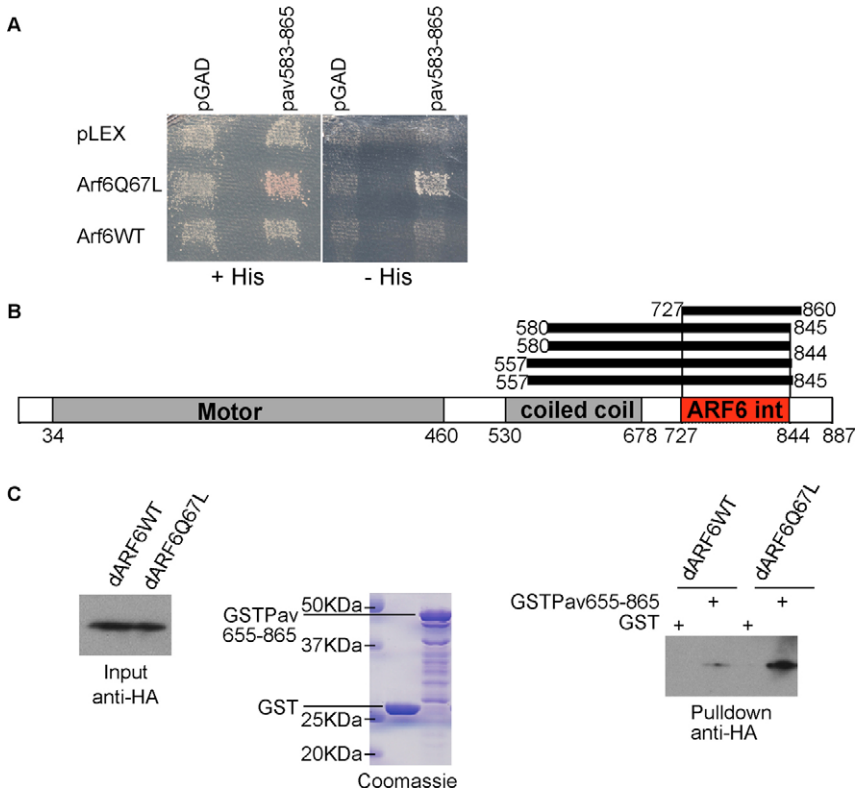

Fig. 7. Physical interaction of Pav and ARF6. (**A**) Growth on medium lacking histidine (–His) indicates a positive two-hybrid interaction of Pav residues 583-865, in the yeast two-hybrid screen with ARF6Q67L. pGAD, pLEX, empty vectors. (**B**) Pav protein domains. Five pav clones interacted with ARF6Q67L in yeast two-hybrid analysis (black bars) defining a minimum overlapping domain (ARF6 int, red). (**C**) Binding assay of ARF6 with Pav. Purified GSTPav655-865, but not GST alone (negative control) pulled down ARF6HA and ARF6Q67LHA from HeLa cell lysates.

amount of endocytic membrane available for recycling. Late regressors might be those cells in which these other components or amounts of available membrane are above a certain threshold level that, if not reached, would lead to early regression. In the late regressors, although membrane addition proceeds at a normal rate, the membrane inserted independently of ARF6 might lack key components that are essential for the stability of the ring canal, and thereby for completion of cytokinesis. Such a defect, which might actually occur throughout cytokinesis, would only manifest itself later by leading to late furrow regression,

Membrane recycling from the central spindle

Is central spindle targeting of recycling endosomes functionally significant? In cleaving *Xenopus* embryos, most membrane insertion occurs next to the furrow (Bluemink and de Laat, 1973). As in *Drosophila* spermatocytes, machinery for fusion of intracellular vesicles with the plasma membrane, including the exocyst complex and syntaxin, is localized to the cleavage furrow and central spindle in many cell types (Fielding et al., 2005; Gromley et al., 2005; Jantsch-Plunger and Glotzer, 1999; Low et al., 2003; VerPlank and Li, 2005). Central spindle proteins may assemble the relevant endocytic and/or secretory factors to facilitate efficient membrane addition. The central spindle might therefore function as a sensor during cytokinesis, implementing membrane trafficking at the right time and, perhaps, at the right place.

Our data showing that ARF6 binds to Pav suggest a possible molecular link between the central spindle and the trafficking machinery. If they are not at the central spindle, both Rab4 and Rab11 recycling endosomes show low levels of ARF6 colocalization during cytokinesis, whereas most of them contain ARF6 when at the spindle. Pav might ensure local enrichment of ARF6 in central spindle endosomes. Indeed, mammalian ARFs bind MKLP1, suggesting Pav-mediated ARF recruitment (Boman et al., 1999). Yeast two-hybrid and GST pull-down experiments confirmed this interaction in *Drosophila*, suggesting that this might be a conserved mechanism in cytokinesis (Fig. 7).

Our data show that in the absence of ARF6, Rab4 recycling endosomes are still targeted to the spindle. Similarly, Rab11 recycling endosomes also reach the central spindle in late *arf6* regressors. It therefore seems that ARF6 and Rab11 are recruited independently, with ARF6 acting downstream of Rab4/Rab11 endosome localization to mediate rapid membrane recycling. Rab11, recruited late to the central spindle, may act in cytokinesis completion as previously suggested (Fielding et al., 2005; Wilson et al., 2005). It has been proposed that ARF6 recruits Rab11 recycling endosomes to the central spindle (Fielding et al., 2005). The contrasting situation in *Drosophila* spermatocytes may be due to the fact that the interaction between ARF6 with human FIP3/4 is not conserved for the *Drosophila* FIP3/4 homologue Nuclear fallout and ARF6 (Wilson et al., 2005).

ARF6-dependent rapid recycling at the central spindle

How does ARF6 boost the recycling rate? One possibility is that ARF6 connects the recycling endosomes concentrated at the central spindle with exocyst-defined fusion sites at the plasma membrane of the cleavage furrow. The exocyst complex localizes to vesicular structures at the central spindle and cleavage furrow, which would be adjacent to the cortical central spindle ARF6 endosomes shown in this report (Fielding et al., 2005; Gromley et al., 2005). ARF6-GTP interacts with the exocyst complex subunit Sec10 (Prigent et al., 2003). ARF6 interaction with the exocyst complex may therefore mediate targeted recycling of membrane to discrete plasma membrane domains (D'Souza-Schorey and Chavrier, 2006). ARF6 might alternatively influence recycling endosome or plasma membrane phospholipid metabolism using the effector phospholipase D, a mechanism frequently implicated in regulated recycling and secretion (Brown et al., 1993; Caumont et al., 1998; Jovanovic et al., 2006; Vitale et al., 2002). Our data suggest that in the absence of ARF6, Rab4/Rab11 endosomes still contribute to a basic rate of membrane recycling, but ARF6 recruitment contributes to more efficient membrane insertion by endowing recycling vesicles with a label to perform directed exocytosis.

Life without ARF6

ARF6 is essential for meiotic cytokinesis in the testes. Occasional spermatids containing more than four nuclei in *arf6* mutants are consistent with cytokinesis failure during the mitosis prior to meiosis in the spermatocytes (Fig. 1). Additionally, karyotyping of third instar homozygous *arf6* larval brains revealed a low but significant frequency of tetraploidy: 4.2±2.2% (n=5 brains, 511 mitosis) in $arf6^{L51b}/arf6^{L51b}$ mutants *versus* 0% (n=4 brains, 385 mitosis) in $arf6^{L51b/+}$ heterozygotes and 0% (n=4 brains, 150 mitosis) in wild-type animals. This suggests a cytokinesis failure during mitosis in this tissue. Furthermore, there is an incompletely penetrant germ line ARF6 requirement during chorion morphogenesis (see Fig. S2 in the supplementary material). However, most somatic mitosis and other developmental processes occur normally in individuals completely lacking ARF6.

Many other *Drosophila* cytokinesis mutants (e.g. *fwd*, *gio*, *klp3A*, *fws*) preferentially affect spermatocyte cytokinesis, with little or no effect on somatic cells (Brill et al., 2000; Farkas et al., 2003; Giansanti et al., 2006; Williams et al., 1995). However, it is surprising that many previously proposed ARF6-dependent processes are not affected in *arf6* maternal/zygotic null mutants. For example, Loner/Schizo, which plays a role during myoblast fusion and axon path finding in *Drosophila* has a specific GEF activity on ARF6, but not ARF1 in vitro, and overexpression of a dominant negative GDP-bound ARF6 mutant partially phenocopies *loner/schizo* mutants (Chen et al., 2003; Onel et al., 2004). The lack of myoblast/neuronal phenotypes of the *arf6* null mutant suggests that the real target of Loner/Schizo is another GTPase or second redundantly acting target.

In mammalian cultured cells, ARF6 mediates essential processes including cell migration, cell-cell adhesion and phagocytosis (D'Souza-Schorey and Chavrier, 2006). The mouse *arf6* knockout shows a developmental phenotype consistent with impaired cell migration during hepatic cord formation (Suzuki et al., 2006). Although we have not analyzed cell adhesion, migration or phagocytosis in detail, *arf6* null mutants survive to the adult stage with no overt morphological defects, which requires all these processes. *Drosophila* has no second *arf6* gene (Lee et al., 1994). The closest homologue encoded in the genome, ARF1 (68% identical), is involved in secretory, but not endocytic trafficking (reviewed in D'Souza-Schorey and Chavrier, 2006). The mouse *arf6* knockout (Suzuki et al., 2006) will tell us in the future whether these functions of ARF6 are vertebrate specific.

The authors thank Peter Foster for writing programs for the cell division model and surface area calculation, and Hybrigenics staff for the yeast two-hybrid analysis. This work was supported by HFSP, DFG, VW and EU grants to M.G.G., RTN-HPRNCT 2002-00260 COMBIO 503568 and SAF 2003-07620 grants to C.G., and a GenHomme Network Grant (02490-6088) to Hybrigenics and Institut Curie.

Supplementary material

Supplementary material for this article is available at http://dev.biologists.org/cgi/content/full/134/24/4437/DC1

References

Adams, R. R., Tavares, A. A., Salzberg, A., Bellen, H. J. and Glover, D. M. (1998). pavarotti encodes a kinesin-like protein required to organize the central spindle and contractile ring for cytokinesis. *Genes Dev*. **12**, 1483-1494.

Albertson, R., Riggs, B. and Sullivan, W. (2005). Membrane traffic: a driving force in cytokinesis. *Trends Cell Biol*. **15**, 92-101.

Amano, M., Ito, M., Kimura, K., Fukata, Y., Chihara, K., Nakano, T., Matsuura, Y. and Kaibuchi, K. (1996). Phosphorylation and activation of myosin by Rho-associated kinase (Rho-kinase). *J. Biol. Chem*. **271**, 20246-20249.

Ang, A. L., Taguchi, T., Francis, S., Folsch, H., Murrells, L. J., Pypaert, M., Warren, G. and Mellman, I. (2004). Recycling endosomes can serve as intermediates during transport from the Golgi to the plasma membrane of MDCK cells. *J. Cell Biol*. **167**, 531-543.

Bartel, P. L. (1993). Using the two-hybrid system to detect protein-protein interactions. In *Cellular Interactions in Development: A Practical Approach* (ed. D. A. Hartley), pp. 153-179. Oxford: Oxford University Press.

Bartel, P., Chien, C. T., Sternglanz, R. and Fields, S. (1993). Elimination of false positives that arise in using the two-hybrid system. *Biotechniques* **14**, 920-924.

Bluemink, J. G. and de Laat, S. W. (1973). New membrane formation during cytokinesis in normal and cytochalasin B-treated eggs of Xenopus laevis. I. Electron microscope observations. *J. Cell Biol*. **59**, 89-108.

Boman, A. L., Kuai, J., Zhu, X., Chen, J., Kuriyama, R. and Kahn, R. A. (1999). Arf proteins bind to mitotic kinesin-like protein 1 (MKLP1) in a GTP-dependent fashion. *Cell Motil. Cytoskeleton* **44**, 119-132.

Boucrot, E. and Kirchhausen, T. (2007). Endosomal recycling controls plasma membrane area during mitosis. *Proc. Natl. Acad. Sci. USA* **104**, 7939-7944.

Brill, J. A., Hime, G. R., Scharer-Schuksz, M. and Fuller, M. T. (2000). A phospholipid kinase regulates actin organization and intercellular bridge formation during germline cytokinesis. *Development* **127**, 3855-3864.

Brown, H. A., Gutowski, S., Moomaw, C. R., Slaughter, C. and Sternweis, P. C. (1993). ADP-ribosylation factor, a small GTP-dependent regulatory protein, stimulates phospholipase D activity. *Cell* **75**, 1137-1144.

Caumont, A. S., Galas, M. C., Vitale, N., Aunis, D. and Bader, M. F. (1998). Regulated exocytosis in chromaffin cells. Translocation of ARF6 stimulates a plasma membrane-associated phospholipase D. *J. Biol. Chem*. **273**, 1373-1379.

Chen, E. H., Pryce, B. A., Tzeng, J. A., Gonzalez, G. A. and Olson, E. N. (2003). Control of myoblast fusion by a guanine nucleotide exchange factor, loner, and its effector ARF6. *Cell* **114**, 751-762.

Chou, T. B. and Perrimon, N. (1992). Use of a yeast site-specific recombinase to produce female germline chimeras in Drosophila. *Genetics* **131**, 643-653.

Clarkson, M. and Saint, R. (1999). A His2AvDGFP fusion gene complements a lethal His2AvD mutant allele and provides an in vivo marker for Drosophila chromosome behavior. *DNA Cell Biol*. **18**, 457-462.

Cooley, L., Verheyen, E. and Ayers, K. (1992). chickadee encodes a profilin required for intercellular cytoplasm transport during Drosophila oogenesis. *Cell* **69**, 173-184.

D'Souza-Schorey, C. and Chavrier, P. (2006). ARF proteins: roles in membrane traffic and beyond. *Nat. Rev. Mol. Cell Biol*. **7**, 347-358.

D'Souza-Schorey, C., Li, G., Colombo, M. I. and Stahl, P. D. (1995). A regulatory role for ARF6 in receptor-mediated endocytosis. *Science* **267**, 1175-1178.

D'Souza-Schorey, C., van Donselaar, E., Hsu, V. W., Yang, C., Stahl, P. D. and Peters, P. J. (1998). ARF6 targets recycling vesicles to the plasma membrane: insights from an ultrastructural investigation. *J. Cell Biol*. **140**, 603-616.

Echard, A., Hickson, G. R., Foley, E. and O'Farrell, P. H. (2004). Terminal cytokinesis events uncovered after an RNAi screen. *Curr. Biol*. **14**, 1685-1693.

Eggert, U. S., Kiger, A. A., Richter, C., Perlman, Z. E., Perrimon, N., Mitchison, T. J. and Field, C. M. (2004). Parallel chemical genetic and genome-wide RNAi screens identify cytokinesis inhibitors and targets. *PLoS Biol*. **2**, e379.

Emery, G., Hutterer, A., Berdnik, D., Mayer, B., Wirtz-Peitz, F., Gaitan, M. G. and Knoblich, J. A. (2005). Asymmetric Rab 11 endosomes regulate delta recycling and specify cell fate in the Drosophila nervous system. *Cell* **122**, 763-773.

Farkas, R. M., Giansanti, M. G., Gatti, M. and Fuller, M. T. (2003). The Drosophila Cog5 homologue is required for cytokinesis, cell elongation, and assembly of specialized Golgi architecture during spermatogenesis. *Mol. Biol. Cell* **14**, 190-200.

Fielding, A. B., Schonteich, E., Matheson, J., Wilson, G., Yu, X., Hickson, G. R., Srivastava, S., Baldwin, S. A., Prekeris, R. and Gould, G. W. (2005). Rab11-FIP3 and FIP4 interact with Arf6 and the exocyst to control membrane traffic in cytokinesis. *EMBO J*. **24**, 3389-3399.

Finger, F. P., Hughes, T. E. and Novick, P. (1998). Sec3p is a spatial landmark for polarized secretion in budding yeast. *Cell* **92**, 559-571.

Formstecher, E., Aresta, S., Collura, V., Hamburger, A., Meil, A., Trehin, A., Reverdy, C., Betin, V., Maire, S., Brun, C. et al. (2005). Protein interaction mapping: a Drosophila case study. *Genome Res*. **15**, 376-384.

Fromont-Racine, M., Rain, J. C. and Legrain, P. (1997). Toward a functional analysis of the yeast genome through exhaustive two-hybrid screens. *Nat. Genet*. **16**, 277-282.

Fuller, M. T. (1993). Spermatogenesis. In *The Development of Drosophila melanogaster* (ed. A. Martinez-Arias and M. Bate), pp. 71-147. Cold Spring Harbor: Cold Spring Harbour Laboratory Press.

Giansanti, M. G., Bonaccorsi, S., Williams, B., Williams, E. V., Santolamazza, C., Goldberg, M. L. and Gatti, M. (1998). Cooperative interactions between the central spindle and the contractile ring during Drosophila cytokinesis. *Genes Dev*. **12**, 396-410.

Giansanti, M. G., Farkas, R. M., Bonaccorsi, S., Lindsley, D. L., Wakimoto, B. T., Fuller, M. T. and Gatti, M. (2004). Genetic dissection of meiotic cytokinesis in Drosophila males. *Mol. Biol. Cell* **15**, 2509-2522.

Giansanti, M. G., Bonaccorsi, S., Kurek, R., Farkas, R. M., Dimitri, P., Fuller, M. T. and Gatti, M. (2006). The class I PITP giotto is required for Drosophila cytokinesis. *Curr. Biol*. **16**, 195-201.

Glotzer, M. (2005). The molecular requirements for cytokinesis. *Science* **307**, 1735-1739.

Gromley, A., Yeaman, C., Rosa, J., Redick, S., Chen, C. T., Mirabelle, S., Guha, M., Sillibourne, J. and Doxsey, S. J. (2005). Centriolin anchoring of exocyst and SNARE complexes at the midbody is required for secretory-vesicle-mediated abscission. *Cell* **123**, 75-87.

Hime, G. R., Brill, J. A. and Fuller, M. T. (1996). Assembly of ring canals in the male germ line from structural components of the contractile ring. *J. Cell Sci.* **109**, 2779-2788.

Jantsch-Plunger, V. and Glotzer, M. (1999). Depletion of syntaxins in the early Caenorhabditis elegans embryo reveals a role for membrane fusion events in cytokinesis. *Curr. Biol*. **9**, 738-745.

Jantsch-Plunger, V., Gonczy, P., Romano, A., Schnabel, H., Hamill, D., Schnabel, R., Hyman, A. A. and Glotzer, M. (2000). CYK-4: A Rho family gtpase activating protein (GAP) required for central spindle formation and cytokinesis. *J. Cell Biol*. **149**, 1391-1404.

Jovanovic, O. A., Brown, F. D. and Donaldson, J. G. (2006). An effector domain mutant of Arf6 implicates phospholipase D in endosomal membrane recycling. *Mol. Biol. Cell* **17**, 327-335.

Kiehart, D. P. and Feghali, R. (1986). Cytoplasmic myosin from Drosophila melanogaster. *J. Cell Biol*. **103**, 1517-1525.

Knutton, S., Sumner, M. C. and Pasternak, C. A. (1975). Role of microvilli in surface changes of synchronized P815Y mastocytoma cells. *J. Cell Biol*. **66**, 568-576.

Lee, F. J., Stevens, L. A., Hall, L. M., Murtagh, J. J., Jr, Kao, Y. L., Moss, J. and Vaughan, M. (1994). Characterization of class II and class III ADP-ribosylation factor genes and proteins in Drosophila melanogaster. *J. Biol. Chem*. **269**, 21555-21560.

Lee, H. S., Simon, J. A. and Lis, J. T. (1988). Structure and expression of ubiquitin genes of Drosophila melanogaster. *Mol. Cell. Biol*. **8**, 4727-4735.

Low, S. H., Li, X., Miura, M., Kudo, N., Quinones, B. and Weimbs, T. (2003). Syntaxin 2 and endobrevin are required for the terminal step of cytokinesis in mammalian cells. *Dev. Cell* **4**, 753-759.

Matsui, T., Amano, M., Yamamoto, T., Chihara, K., Nakafuku, M., Ito, M., Nakano, T., Okawa, K., Iwamatsu, A. and Kaibuchi, K. (1996). Rho-associated kinase, a novel serine/threonine kinase, as a putative target for small GTP binding protein Rho. *EMBO J*. **15**, 2208-2216.

Minestrini, G., Harley, A. S. and Glover, D. M. (2003). Localization of Pavarotti-KLP in living Drosophila embryos suggests roles in reorganizing the cortical cytoskeleton during the mitotic cycle. *Mol. Biol. Cell* **14**, 4028-4038.

Needham, D. and Hochmuth, R. M. (1989). Electro-mechanical permeabilization of lipid vesicles. Role of membrane tension and compressibility. *Biophys. J*. **55**, 1001-1009.

Oda, H. and Tsukita, S. (2001). Real-time imaging of cell-cell adherens junctions reveals that Drosophila mesoderm invagination begins with two phases of apical constriction of cells. *J. Cell Sci.* **114**, 493-501.

Onel, S., Bolke, L. and Klambt, C. (2004). The Drosophila ARF6-GEF Schizo controls commissure formation by regulating Slit. *Development* **131**, 2587-2594.

Pelissier, A., Chauvin, J. P. and Lecuit, T. (2003). Trafficking through Rab11 endosomes is required for cellularization during Drosophila embryogenesis. *Curr. Biol*. **13**, 1848-1857.

Prigent, M., Dubois, T., Raposo, G., Derrien, V., Tenza, D., Rosse, C., Camonis, J. and Chavrier, P. (2003). ARF6 controls post-endocytic recycling through its downstream exocyst complex effector. *J. Cell Biol*. **163**, 1111-1121.

Radhakrishna, H. and Donaldson, J. G. (1997). ADP-ribosylation factor 6 regulates a novel plasma membrane recycling pathway. *J. Cell Biol*. **139**, 49-61.

Rebollo, E. and Gonzalez, C. (2004). Time-lapse imaging of male meiosis by phase-contrast and fluorescence microscopy. *Methods Mol. Biol*. **247**, 77-87.

Rebollo, E., Llamazares, S., Reina, J. and Gonzalez, C. (2004). Contribution of noncentrosomal microtubules to spindle assembly in Drosophila spermatocytes. *PLoS Biol*. **2**, E8.

Royou, A., Field, C., Sisson, J. C., Sullivan, W. and Karess, R. (2004).

Reassessing the role and dynamics of nonmuscle myosin II during furrow formation in early Drosophila embryos. *Mol. Biol. Cell* **15**, 838-850.
Salzberg, A., D'Evelyn, D., Schulze, K. L., Lee, J. K., Strumpf, D., Tsai, L. and Bellen, H. J. (1994). Mutations affecting the pattern of the PNS in Drosophila reveal novel aspects of neuronal development. *Neuron* **13**, 269-287.
Satoh, N. and Deno, T. (1984). Periodic appearance and disappearance of microvilli associated with cleavage cycles in the egg of the ascidian, Halocynthia roretzi. *Dev. Biol*. **102**, 488-492.
Schweitzer, J. K. and D'Souza-Schorey, C. (2002). Localization and activation of the ARF6 GTPase during cleavage furrow ingression and cytokinesis. *J. Biol. Chem*. **277**, 27210-27216.
Schweitzer, J. K. and D'Souza-Schorey, C. (2005). A requirement for ARF6 during the completion of cytokinesis. *Exp. Cell Res*. **311**, 74-83.
Sheff, D. R., Daro, E. A., Hull, M. and Mellman, I. (1999). The receptor recycling pathway contains two distinct populations of early endosomes with different sorting functions. *J. Cell Biol*. **145**, 123-139.
Skop, A. R., Bergmann, D., Mohler, W. A. and White, J. G. (2001). Completion of cytokinesis in C. elegans requires a brefeldin A-sensitive membrane accumulation at the cleavage furrow apex. *Curr. Biol*. **11**, 735-746.
Skop, A. R., Liu, H., Yates, J., 3rd, Meyer, B. J. and Heald, R. (2004). Dissection of the mammalian midbody proteome reveals conserved cytokinesis mechanisms. *Science* **305**, 61-66.
Somers, W. G. and Saint, R. (2003). A RhoGEF and Rho family GTPase-activating protein complex links the contractile ring to cortical microtubules at the onset of cytokinesis. *Dev. Cell* **4**, 29-39.
Song, J., Khachikian, Z., Radhakrishna, H. and Donaldson, J. G. (1998). Localization of endogenous ARF6 to sites of cortical actin rearrangement and involvement of ARF6 in cell spreading. *J. Cell Sci.* **111**, 2257-2267.
Suzuki, T., Kanai, Y., Hara, T., Sasaki, J., Sasaki, T., Kohara, M., Maehama, T., Taya, C., Shitara, H., Yonekawa, H. et al. (2006). Crucial role of the small GTPase ARF6 in hepatic cord formation during liver development. *Mol. Cell. Biol*. **26**, 6149-6156.
van der Sluijs, P., Hull, M., Webster, P., Male, P., Goud, B. and Mellman, I. (1992). The small GTP-binding protein rab4 controls an early sorting event on the endocytic pathway. *Cell* **70**, 729-740.
VerPlank, L. and Li, R. (2005). Cell cycle-regulated trafficking of Chs2 controls actomyosin ring stability during cytokinesis. *Mol. Biol. Cell* **16**, 2529-2543.
Vitale, N., Chasserot-Golaz, S. and Bader, M. F. (2002). Regulated secretion in chromaffin cells: an essential role for ARF6-regulated phospholipase D in the late stages of exocytosis. *Ann. N. Y. Acad. Sci*. **971**, 193-200.
Vojtek, A. B. and Hollenberg, S. M. (1995). Ras-Raf interaction: two-hybrid analysis. *Meth. Enzymol*. **255**, 331-342.
Williams, B. C., Riedy, M. F., Williams, E. V., Gatti, M. and Goldberg, M. L. (1995). The Drosophila kinesin-like protein KLP3A is a midbody component required for central spindle assembly and initiation of cytokinesis. *J. Cell Biol*. **129**, 709-723.
Wilson, G. M., Fielding, A. B., Simon, G. C., Yu, X. Andrews, P. D., Hames, R. S., Frey, A. M., Peden, A. A., Gould, G. W. and Prekeris, R. (2005). The FIP3-Rab11 protein complex regulates recycling endosome targeting to the cleavage furrow during late cytokinesis. *Mol. Biol. Cell* **16**, 849-860.
Wucherpfennig, T., Wilsch-Brauninger, M. and Gonzalez-Gaitan, M. (2003). Role of Drosophila Rab5 during endosomal trafficking at the synapse and evoked neurotransmitter release. *J. Cell Biol*. **161**, 609-624.
Xu, H., Brill, J. A., Hsien, J., McBride, R., Boulianne, G. L. and Trimble, W. S. (2002). Syntaxin 5 is required for cytokinesis and spermatid differentiation in Drosophila. *Dev. Biol*. **251**, 294-306.
Yamashiro, S., Totsukawa, G., Yamakita, Y., Sasaki, Y., Madaule, P., Ishizaki, T., Narumiya, S. and Matsumura, F. (2003). Citron kinase, a Rho-dependent kinase, induces di-phosphorylation of regulatory light chain of myosin II. *Mol. Biol. Cell* **14**, 1745-1756.